Stair Matrix and its Applications to Massive MIMO Uplink Data Detection

Fan Jiang, *Student Member, IEEE,* Cheng Li, *Senior Member, IEEE,* Zijun Gong, *Senior Member, IEEE,* and Ruoyu Su, *Student Member, IEEE*

***Abstract*—In this paper, we propose a new approach of using the stair matrix for uplink data detection in massive MIMO systems. We first demonstrate the applicability of the proposed method by showing that the probability (that the convergence conditions are met) will approach one as long as sufficient large number of antennas are equipped at the base station. We then propose an iterative method to perform data detection and show that a much improved performance can be achieved with the computational complexity remaining at the same level of existing iterative methods where the diagonal matrix is adopted. Performance evaluation is conducted in terms of the probability that the convergence conditions are met, the normalized mean-square error of the Neumann series expansion to approach the matrix inverse, the residual estimation error to approach the linear ZF/MMSE detection, and the system bit error rate. Numerical simulations show significant performance enhancement of using the stair matrix over the diagonal matrix in all performance aspects.**

***Index Terms*—Massive MIMO; Stair Matrix; Iterative Method; Convergence Condition.**

I. Introduction

The development and successful applications of multiple-input multiple-output (MIMO) systems in modern wireless communications have brought the bright prospective of massive MIMO techniques in future 5G mobile communication systems [1]–[3]. It is foreseeable that massive MIMO, together with the millimeter wave frequency band [4], has been a promising candidate to meet the high rate, low latency 5G system requirements. Due to the huge potential multiplexing and diversity gain over the small-scale MIMO and single-antenna systems, massive MIMO can boom the system spectrum and energy efficiency [1], [5]–[7]. Along with the benefits of massive MIMO, however, the cost of high computational complexity required in signal processing (data detection, precoding, etc.) increases, which prohibits the application of the optimal detection methods, such as the maximum likelihood (ML), and maximum *a posteriori* (MAP) detection, in realization.

To achieve good tradeoff between the system performance and the computational complexity, linear detection (and precoding) methods, such as zero-forcing (ZF) and minimum mean-square error (MMSE), have been considered in realization [8]–[15]. It has also been demonstrated that with these linear detection methods, the near-optimal performance can be achieved in massive MIMO systems, especially when the number of antennas at base station (denoted by N_B) is much greater than the number of user equipment (denoted by N_U) in service. However, as we know, ZF/MMSE based data detection schemes experience matrix inversion, which is computational costly (almost $\mathcal{O}\left(N^3\right)$, where N is the matrix size) in implementation. Therefore, the investigation of reducing computational complexity but still maintaining near-optimal system performance of ZF/MMSE based data detection schemes has emerged recently [8]–[15]. Generally, all those schemes can be summarized in two categories: the first one is to approach matrix inversion, and the other is to solve linear equations with iterative methods.

The first category is to approach the matrix inversion [8]–[10]. For example, in [8], the authors attempt to introduce Neumann series expansion to avoid the matrix inversion in linear MMSE detection. It has been shown that when the number of antennas at base station is much greater than the number of user equipment, the orders required for Neumann series expansion can be as few as 3 (for example, $r = N_B/N_U \geqslant 16$). In [9], the probability of the convergence condition that using the diagonal matrix in Neumann series expansion has been comprehensively discussed. However, Neumann series expansion suffers from matrix multiplications, and the computational complexity is comparable to the matrix inversion algorithm when the expansion order is more than two. In order to speed up the convergence rate, diagonal banded Newton iteration based matrix inversion approach is studied in [10], where the Newton iteration structure is used. Actually, the results after P iterations in Newton iteration can be seen as the Neumann series expansion of the order $2^P - 1$ [10]. Inevitably, matrix multiplications are involved in diagonal banded Newton iteration based matrix inversion approach, and the iterations are limited to 2 for computational complexity consideration. In summary, the methods that are to approach matrix inversion suffer from high computational complexity due to the matrix multiplications and the slow convergence rate when the ratio r is not sufficiently large.

The second category is to solve linear equations with iterative methods [11]–[15]. The basic idea of these methods is to transform the matrix inversion problem into solving linear equations. To solve the linear equations, an initial estimation is provided. Then following an iterative structure to converge, the final output is provided as the solutions to linear equations. For example, in [11], the Jacobi method is adopted, and by following the Jacobi iterative structure, the estimation eventually approaches the MMSE estimation. The Richardson

The authors are with the Department of Electrical and Computer Engineering, Faculty of Engineering and Applied Science, Memorial University of Newfoundland, St. John's, NL, A1B 3X5, Canada.

E-mail: {fjiang, licheng, zg7454}@mun.ca

iteration in massive MIMO uplink data detection has been studied in [12], and the authors have demonstrated that the iterative structure can converge even with zero initialization. However, as pointed out in [13], [14], the convergence rate for both Jacobi method and Richardson iteration is slow, hence quite a few iterations are required for convergence. The application of Gauss-Seidel method to massive MIMO uplink data detection is studied in [13], and the convergence performance can be greatly improved. By providing an initial estimation that is close to the MMSE estimation, the joint steepest-decent and Jacobi method based data detection is proposed in [14], and the iterations are greatly reduced. In [15], the authors formulate the MMSE estimation as a minimization problem, and use the conjugate gradient to calibrate the next estimation. However, conjugate gradient-based data detection scheme involves many division operations, which is also computational costly. Compared to the first category which is to approach matrix inversion, solving linear equations with iterative methods is of less complexity due to the replacement of matrix multiplications with matrix-vector products. However, as summarized in [14], the overall computational complexity of the iterative methods, including the computations in both the initialization and iteration, is still high. It is worth pointing out that the convergence rate of the existing iterative methods can be speeded up by using preconditioning [16]. The potential direction to further reduce the computational complexity can be finding an iterative method that requires less computation in initialization and less iterations for convergence [17].

In both the previous mentioned two categories of data detection schemes, we note that most proposals in existing literatures mainly utilize the diagonal matrix in the development. In [8], [9], the applicability of using diagonal matrix to massive MIMO uplink data detection has been demonstrated. However, as we will show later, we find some limitations for using diagonal matrix. First of all, in the massive MIMO system configuration with small ratio of $r = N_B/N_U$, the convergence rate of using the diagonal matrix is slow. Alternatively, a few iterations (or orders in Neumann series expansion) are required to provide near-optimal system performance. Besides, the convergence conditions, which are critical for the both data detection schemes mentioned above, are met with a low probability when r is small. That is to say, in some cases, the diagonal matrix may not be used to converge.

The motivation of this paper originates from achieving a better tradeoff between computational complexity and system performance in massive MIMO uplink data detection. We propose to use the stair matrix in the development. As far as we know, the applications of stair matrix in massive MIMO systems have not been studied. The contributions of this paper are summarized as follows:

- We show that when N_B grows to infinite, the probability that the convergence conditions are met approaches 1. As the antennas at base station in Massive MIMO systems can be hundreds, this conclusion demonstrates the applicability of the stair matrix in massive MIMO systems;
- We demonstrate the proposed iterative method with the use of the stair matrix has the same level of the computational complexity compared to the existing iterative methods where the diagonal matrix is applied;
- We show that by using the stair matrix, the probability that the convergence conditions are met can be greatly improved in a comparatively low r region, and the cumulative distribution function of the maximum eigenvalue of the convergence matrix indicates that the convergence rate can be speeded up by using the stair matrix;
- We demonstrate that by using the stair matrix, the mean-square error of the truncated Neumann series expansion to approach matrix inverse, can be greatly reduced;
- We show that the residual estimation error of the proposed iterative method using the stair matrix is much less than that of the Jacobi method where the diagonal matrix is applied;
- We compare the system BER performance with the proposed iterative method, and show that the performance improvement over the use of the diagonal matrix is significant.

The rest of this paper is organized as follows. Section II provides the system model, including the massive MIMO structure and the preliminary work of linear ZF/MMSE detection. In section III, the introduction to stair matrix and its applicability in massive MIMO will be presented. The implementation of stair matrix in massive MIMO data detection with iterative method is presented in section IV. In section V, we conduct the numerical simulations and present the results and discussion. Finally, the conclusions are drawn in section VI.

Notations: Throughout the paper, the lowercase and uppercase bold symbols denote the column vector and matrix, respectively. $(\cdot)^{\mathrm{T}}$, $(\cdot)^{\mathrm{H}}$, and $(\cdot)^{-1}$ are reserved for matrix transpose, conjugate transpose, and inverse, respectively. $\mathbb{C}$ and $\mathbb{N}$ are reserved for the sets of the complex and natural numbers, respectively. $\|\mathbf{A}\|_{\mathrm{F}}$ and $\|\mathbf{a}\|_2$ are the Frobenius-norm of a matrix $\mathbf{A}$ and the ℓ_2-norm of a vector $\mathbf{a}$. $\mathrm{E}\{\cdot\}$ and $\mathrm{cov}\{\cdot,\cdot\}$ denote the expectation, and covariance operation. $\exp(\cdot)$ and $\ln(\cdot)$ denote the exponential and natural logarithmic functions, respectively. $\mathbf{I}_L$ is reserved for the size L identity matrix and $\mathbf{e}_l$ represents the lth column of $\mathbf{I}_L$; $\mathrm{diag}\{\mathbf{a}\}$ converts a column vector $\mathbf{a}$ to a diagonal matrix and $\mathrm{diag}\{\mathbf{A}\}$ obtains the diagonal elements in a matrix $\mathbf{A}$ to form a column vector. $\rho(\mathbf{A})$ is the spectral radius of the matrix $\mathbf{A}$.

II. System Model

We consider the massive MIMO uplink with N_B antennas at base station to simultaneously serve N_U single-antenna user equipment. The N_B bitstream from each user is first encoded, then interleaved, and fed into digital modulator. The modulated symbols are transmitted into massive MIMO channel, and the received signal vector at base station can be expressed as

$$\mathbf{y} = \mathbf{H}\mathbf{x} + \mathbf{z}, \tag{1}$$

where $\mathbf{y} = [y_1, y_2, \cdots, y_{N_B}]^{\mathrm{T}}$ is a complex-valued $N_B \times 1$ vector, with y_m denoting the received signal from the m-th receiving antenna. $\mathbf{x} = [x_1, x_2, \cdots, x_{N_U}]^{\mathrm{T}}$ with the transmitted symbol of user u denoted by x_u. $\mathbf{H} = [\mathbf{h}_1, \mathbf{h}_2, \cdots, \mathbf{h}_{N_U}]$ denotes the channel matrix with $\mathbf{h}_u \in \mathbb{C}^{N_B \times 1}$ where each entry is independent and identically distributed (i.i.d.), modeled as the flat

Rayleigh fading channel [1], [5], [13]. $\mathbf{z} = \left[z_1, z_2, \cdots, z_{N_B}\right]^{\mathrm{T}}$ is the noise vector, satisfying $\mathrm{E}\left\{\mathbf{z}\mathbf{z}^{\mathrm{H}}\right\} = \sigma_z^2 \mathbf{I}_{N_B}$ with each entry modeled as zero-mean complex Gaussian circularly symmetric (ZMCGCS) random variable. It is worth noting that in frequency selective fading channels, by applying the OFDM/SC-FDMA techniques, the signal model expressed in (1) is applied to each subcarrier.

A. Linear MMSE Data Detection

The multi-user data detector at the base station is to compute the *a posteriori* log likelihood ratio (LLR) of the bits associated with the modulated symbols. After the knowledge of the channel matrix (note that the channel matrix is obtained through channel estimator, where time domain and/or frequency domain training pilots are used for the channel estimation [18], [19]), the well-known linear MMSE data detection can be given by

$$\hat{\mathbf{x}} = \left(\mathbf{H}^{\mathrm{H}}\mathbf{H} + \sigma_z^2 \mathbf{I}_{N_U}\right)^{-1} \mathbf{H}^{\mathrm{H}}\mathbf{y} = \mathbf{W}^{-1}\mathbf{y}^{\mathrm{MF}}, \tag{2}$$

where $\mathbf{y}^{\mathrm{MF}} = \mathbf{H}^{\mathrm{H}}\mathbf{y}$ can be seen as the matched-filter output, and the MMSE equalization matrix $\mathbf{W}$ can be expressed as

$$\mathbf{W} = \mathbf{G} + \sigma_z^2 \mathbf{I}_{N_U}, \tag{3}$$

where $\mathbf{G} = \mathbf{H}^{\mathrm{H}}\mathbf{H}$ is the Gram matrix. It is worth noting that in high signal-to-noise ratio (SNR) region, Equation (2) can be reduced to

$$\hat{\mathbf{x}} = \mathbf{G}^{-1}\mathbf{y}^{\mathrm{MF}}, \tag{4}$$

which is the linear ZF data detection scheme, where the noise component is not considered in the equalization process.

To obtain the *a posteriori* LLR of the bits associated with the modulated symbols, we write the estimation in Equation (2) as

$$\hat{x}_u = \mathbf{e}_u^{\mathrm{H}}\hat{\mathbf{x}} = \rho_u x_u + \xi_u, \tag{5}$$

where the equivalent channel gain ρ_u and the *a posteriori* noise-plus-interference (NPI) ξ_u can be given by

$$\rho_u = \mathbf{e}_u^{\mathrm{H}}\mathbf{W}^{-1}\mathbf{G}\mathbf{e}_u, \tag{6}$$

$$\xi_u = \mathbf{e}_u^{\mathrm{H}}\mathbf{W}^{-1}\mathbf{G}\left(\mathbf{x} - x_u\mathbf{e}_u\right) + \mathbf{e}_u^{\mathrm{H}}\mathbf{W}^{-1}\mathbf{H}^{\mathrm{H}}\mathbf{z}. \tag{7}$$

The covariance of the NPI $v_u^2 = \mathrm{cov}\left(\xi_u, \xi_u\right)$ is given by

$$\begin{aligned} v_u^2 &= \mathbf{e}_u^{\mathrm{H}}\mathbf{W}^{-1}\mathbf{G}\mathbf{G}\mathbf{W}^{-1}\mathbf{e}_u + \sigma_z^2\mathbf{e}_u^{\mathrm{H}}\mathbf{W}^{-1}\mathbf{G}\mathbf{W}^{-1}\mathbf{e}_u - \rho_u^2 \\ &= \rho_u - \rho_u^2. \end{aligned} \tag{8}$$

Given Equation (5), (6), and (8), we derive the max-log approximated LLR of the bits associated with x_u, given by

$$L\left(b_{u,k}\right) = \gamma_u \left(\min_{s \in \chi_k^0} \left|\frac{\hat{x}_u}{\rho_u} - s\right|^2 - \min_{s' \in \chi_k^1} \left|\frac{\hat{x}_u}{\rho_u} - s'\right|^2\right), \tag{9}$$

where $b_{u,k}$ is the k-th mapping bit associated with x_u; $\gamma_u = \rho_u^2 / v_u^2$ is the *a posteriori* signal-to-noise-plus-interference ratio (SINR); $\chi_k^b \triangleq \left\{s \left| s \in \chi, q_k = b\right.\right\}$ denotes the subset of χ, where the k-th mapping bit associated with the constellation symbol s, i.e. q_k, is b; χ is the constellation symbols set. After data detection of all users, the LLRs are fed into the soft-input channel decoder for decoding process.

B. Neumann Series Expansion

In the previous subsection, we note that the matrix inverse operations are involved in linear MMSE/ZF data detection. The matrix inverse is computational costly especially when the matrix size is large. One of the promising practical solutions to address the matrix inverse issue is to employ the Neumann series expansion [8]. The complete Neumann series expansion of the matrix inverse $\mathbf{W}^{-1}$ is given by

$$\mathbf{W}^{-1} = \sum_{l=0}^{\infty} \left(\mathbf{X}^{-1}\left(\mathbf{X} - \mathbf{W}\right)\right)^l \mathbf{X}^{-1}, \tag{10}$$

with the following condition satisfied:

$$\lim_{l \to \infty} \left(\mathbf{I} - \mathbf{X}^{-1}\mathbf{W}\right)^l = \mathbf{0}. \tag{11}$$

When the high order is ignored, the truncated Neumann series expansion can be expressed as

$$\mathbf{W}_L^{-1} = \sum_{l=0}^{L-1} \left(\mathbf{X}^{-1}\left(\mathbf{X} - \mathbf{W}\right)\right)^l \mathbf{X}^{-1}. \tag{12}$$

Generally, when we select the matrix $\mathbf{X}$ that is close to $\mathbf{W}$, the L order expansion $\mathbf{W}_L^{-1}$ in Equation (12) can be close to $\mathbf{W}^{-1}$. Fortunately, in massive MIMO systems, the gram matrix $\mathbf{G}$ is diagonally dominant; hence the diagonal matrix, i.e., $\mathbf{D} = \mathrm{diag}\left\{\mathbf{W}\right\}$ can be selected as $\mathbf{X}$, then the approximation of $\mathbf{W}^{-1}$ is given by

$$\mathbf{W}_L^{-1} = \sum_{l=0}^{L-1} \left(\mathbf{D}^{-1}\left(\mathbf{D} - \mathbf{W}\right)\right)^l \mathbf{D}^{-1}. \tag{13}$$

In [8], the authors have provided the upper bound of the residual estimation error using $\mathbf{W}_L^{-1}$ to approach $\mathbf{W}^{-1}$, i.e.,

$$\left\|\left(\mathbf{W}^{-1} - \mathbf{W}_L^{-1}\right)\mathbf{y}^{\mathrm{MF}}\right\|_2 \leqslant \left\|\mathbf{I} - \mathbf{D}^{-1}\mathbf{W}\right\|_{\mathrm{F}}^L \left\|\hat{\mathbf{x}}\right\|_2, \tag{14}$$

where $\|\mathbf{A}\|_{\mathrm{F}}$ and $\|\mathbf{a}\|_2$ are the Frobenius norm of a matrix $\mathbf{A}$ and the ℓ_2-norm of a vector $\mathbf{a}$. From Equation (14), we can see that the upper bound of residual estimation error decreases as the increase of the expansion order and N_B. In other words, if the number of antennas at the base station is sufficiently large, even with a small order expansion, the residual estimation error will be small. Particularly, when N_B is sufficient large and the expansion order $L \leqslant 2$, the computation required for the Neumann series expansion will be much reduced, compared to the matrix inverse operations. These two factors provide the evidence to support the usage of the diagonal matrix in Neumann series expansion for massive MIMO systems.

C. Jacobi Method

In Neumann series expansion, if the expansion order is greater than 2, the matrix multiplication operations are involved; hence, the computational complexity is comparable with that of the matrix inverse operations. On the other hand, as we can see in Equation (14), if N_B is not sufficiently large, with the expansion order that is less than 2, the residual estimation error is still considerable. These two factors limit the applications of diagonal matrix in Neumann series expansion.

To avoid the matrix multiplication operations, but maintain a reasonable orders of expansion, we can use the iterative methods. To be specific, we first rewrite the MMSE estimation in Equation (2) as

$$\mathbf{W}\hat{\mathbf{x}} = \mathbf{y}^{\mathrm{MF}}. \tag{15}$$

By transforming the matrix inverse problem into the format of Equation (15), we can adopt the iterative methods to solve linear equations. Generally, the iterative methods follow the following process:

(1) Provide an initial estimation;
(2) Follow an iterative structure to obtain the next estimation;
(3) When the estimation converges, output the final estimation.

In Jacobi method, we can have the initial estimation as

$$\mathbf{x}^{(0)} = \mathbf{D}^{-1}\mathbf{y}^{\mathrm{MF}}, \tag{16}$$

which is the common selection in most of the existing literature. The iterative structure is given by

$$\begin{aligned}\mathbf{x}^{(i+1)} &= \mathbf{D}^{-1}\left((\mathbf{D}-\mathbf{W})\,\mathbf{x}^{(i)} + \mathbf{y}^{\mathrm{MF}}\right)\\ &= \mathbf{x}^{(i)} - \mathbf{D}^{-1}\mathbf{W}\mathbf{x}^{(i)} + \mathbf{D}^{-1}\mathbf{y}^{\mathrm{MF}},\end{aligned} \tag{17}$$

where $\mathbf{x}^{(i)}$ denotes the i-th estimation. According to the iterative structure in Equation (17), and use the initial estimation given by Equation (16), we can derive the i-th estimation given by

$$\mathbf{x}^{(i)} = \sum_{l=0}^{i}\left(\mathbf{D}^{-1}(\mathbf{D}-\mathbf{W})\right)^{l}\mathbf{D}^{-1}\mathbf{y}^{\mathrm{MF}}. \tag{18}$$

That is to say, by selecting the initial estimation given by (16), after i iterations following Jacobi iterative structure, we have the same estimation results as the $(i+1)$-th order expansion in Neumann series. Therefore, the convergence conditions, the residual estimation error, and the estimation results are the same as those in the previous subsection. However, as we can see from Equation (16) to Equation (17), only matrix-vector product operations are involved; therefore, Jacobi method has low complexity compared to the Neumann series expansion with the same iterations (or orders in Neumann series).

III. Stair Matrix and its Applicability to Massive MIMO Systems

In this section, we will first introduce the stair matrix and its properties. And then, we will demonstrate the applicability of the stair matrix to massive MIMO systems.

A. Stair Matrix and its Properties

In an $N\times N$ matrix $\mathbf{A}$, if its entry $\mathbf{A}_{(m,n)} = \mathbf{e}_m^H\mathbf{A}\mathbf{e}_n$, $m,n = 1,2,\cdots,N$, satisfies $\mathbf{A}_{(m,n)} = 0$ where $n \notin [m-1,m,m+1]$, we then call it as a tridiagonal matrix, denoted by $\mathbf{A} = \mathrm{tridiag}\left(\mathbf{A}_{(m,m-1)},\mathbf{A}_{(m,m)},\mathbf{A}_{(m,m+1)}\right)$. A special tridiagonal matrix is defined as a stair matrix if one of the following conditions is satisfied [20], [21]:

(I) $\mathbf{A}_{(m,m-1)} = 0$, $\mathbf{A}_{(m,m+1)} = 0$, where $m = 2k-1$, $k = 1,2,\cdots,\lfloor (N+1)/2\rfloor$;

Algorithm 1: Compute the Inverse of a Stair Matrix

Input: The Stair Matrix $\mathbf{A} = \mathrm{stair}\left(\mathbf{A}_{(m,m-1)},\mathbf{A}_{(m,m)},\mathbf{A}_{(m,m+1)}\right)$
Output: $\mathbf{A}^{-1} = \mathbf{B} = \mathrm{stair}\left(\mathbf{B}_{(m,m-1)},\mathbf{B}_{(m,m)},\mathbf{B}_{(m,m+1)}\right)$
for $m = 1:1:N$
  $\mathbf{B}_{(m,m)} = 1/\mathbf{A}_{(m,m)}$
end
for $m = 2:2:2\lfloor N/2\rfloor$
  $\mathbf{B}_{(m,m-1)} = -\mathbf{A}_{(m,m-1)}\mathbf{B}_{(m,m)}\mathbf{B}_{(m-1,m-1)}$;
  $\mathbf{B}_{(m,m+1)} = -\mathbf{A}_{(m,m+1)}\mathbf{B}_{(m,m)}\mathbf{B}_{(m+1,m+1)}$;
end
Return $\mathbf{B}$.

(II) $\mathbf{A}_{(m,m-1)} = 0$, $\mathbf{A}_{(m,m+1)} = 0$, where $m = 2k$, $k = 1,2,\lfloor N/2\rfloor$.

In accordance, a stair matrix is of type I if the condition (I) is satisfied and is of type II if the condition (II) is satisfied. For example, a 5×5 stair matrix has the following forms:

$$\mathbf{A} = \begin{bmatrix} \times & & & & \\ \times & \times & \times & & \\ & & \times & & \\ & & \times & \times & \times \\ & & & & \times \end{bmatrix} \text{ or } \mathbf{A} = \begin{bmatrix} \times & \times & & & \\ & \times & & & \\ & \times & \times & \times & \\ & & & \times & \\ & & & \times & \times \end{bmatrix}.$$

The previous one is of type I and the latter one is of type II. Next, we provide the following properties of the stair matrix in ***Corollary*** 1 and 2.

Corollary 1: Let $\mathbf{A}$ be a stair matrix. Then $\mathbf{A}^{\mathrm{H}}$ is also a stair matrix. In addition, if $\mathbf{A}$ is of type I, then $\mathbf{A}^{\mathrm{H}}$ is of type II, and vice verse.

Proof: Using the definition, it is straightforward to obtain *Corollary* 1. ■

Corollary 1 shows that the properties of the stair matrix of type I and type II are almost the same; therefore, we only consider the stair matrix of type I hereafter except for specification.

Corollary 2: Let $\mathbf{A}$ be a stair matrix. $\mathbf{A}$ is nonsingular if and only if $\mathbf{A}_{m,m}$, $m = 1,2,\cdots,N$, is nonsingular. Furthermore, the inverse of $\mathbf{A}$, i.e., $\mathbf{A}^{-1}$ is also a stair matrix of the same type, given by $\mathbf{A}^{-1} = \mathbf{D}^{-1}(2\mathbf{D}-\mathbf{A})\mathbf{D}^{-1}$, where $\mathbf{D} = \mathrm{diag}(\mathbf{A})$.

Proof: Since $\det(\mathbf{A}) = \prod_{m=1}^{N}\mathbf{A}_{(m,m)}$, we can see that $\mathbf{A}$ is nonsingular if and only if $\mathbf{A}_{(m,m)}$, $m = 1,2,\cdots,N$, is nonsingular.

Following the matrix multiplications, we can obtain that $\mathbf{D}^{-1}(2\mathbf{D}-\mathbf{A})\mathbf{D}^{-1}\mathbf{A} = \mathbf{I}_N$. Moreover, we can easily derive that $\mathbf{A}^{-1}$ is also a stair matrix and of the same type as $\mathbf{A}$. ■

Without loss of generalness, we denote a stair matrix of type I as $\mathbf{A} = \mathrm{stair}\left(\mathbf{A}_{(m,m-1)},\mathbf{A}_{(m,m)},\mathbf{A}_{(m,m+1)}\right)$. From *Corollary* 2, we have the **Algorithm 1** to obtain $\mathbf{A}^{-1}$. It is clear from **Algorithm 1** that the complexity to obtain the inverse of a stair matrix is $\mathcal{O}(N)$, which is the same order of the computation of $\mathbf{D}^{-1}$.

B. Using Stair Matrix in Neumann Series Expansion

We define the stair matrix $\mathbf{S} = \mathrm{stair}\left(\mathbf{G}_{u,u-1},\mathbf{G}_{u,u},\mathbf{G}_{u,u+1}\right)$, derived from Gram matrix $\mathbf{G}$ as

$$\mathbf{S}_{(u,v)} = \begin{cases} \mathbf{G}_{(u,v)}, & u\in\mathbb{U}_1, v = u;\\ \mathbf{G}_{(u,v)}, & u\in\mathbb{U}_2, v\in\{u-1,u,u+1\};\\ 0, & \text{otherwise},\end{cases}$$

$$\mathbf{B}_{(u,v)} = \begin{cases} -\frac{\mathbf{G}_{(u,v)}}{\mathbf{G}_{(u,u)}}, & u \in \mathbb{U}_1, v \neq u; \\ 0, & u \in \mathbb{U}_1, v = u; \\ -\frac{\mathbf{G}_{(u,v)}}{\mathbf{G}_{(u,u)}} + \frac{\mathbf{G}_{(u,u-1)} \cdot \mathbf{G}_{(u-1,v)}}{\mathbf{G}_{(u,u)} \mathbf{G}_{(u-1,u-1)}} + \frac{\mathbf{G}_{(u,u+1)} \cdot \mathbf{G}_{(u+1,v)}}{\mathbf{G}_{(u,u)} \mathbf{G}_{(u+1,u+1)}}, & u \in \mathbb{U}_2, v \neq u; \\ \frac{\mathbf{G}_{(u,u-1)} \cdot \mathbf{G}_{(u-1,u)}}{\mathbf{G}_{(u,u)} \mathbf{G}_{(u-1,u-1)}} + \frac{\mathbf{G}_{(u,u+1)} \cdot \mathbf{G}_{(u+1,u)}}{\mathbf{G}_{(u,u)} \mathbf{G}_{(u+1,u+1)}}, & u \in \mathbb{U}_2, v = u. \end{cases} \tag{22}$$

where $\mathbb{U} \triangleq \{n | n \in \mathbb{N}, n \leqslant N_U\}$; $\mathbb{U}_1$ and $\mathbb{U}_2$ are subsets of $\mathbb{U}$, defined as $\mathbb{U}_1 \triangleq \{n | n \in \mathbb{U}, n = 2k-1, k \in \mathbb{N}\}$, and $\mathbb{U}_2 \triangleq \{n | n \in \mathbb{U}, n = 2k, k \in \mathbb{N}\}$, respectively.

Applying the stair matrix in Neumann series expansion in Equation (10), we have [1]

$$\mathbf{G}^{-1} = \sum_{k=0}^{\infty} \left(\mathbf{I} - \mathbf{S}^{-1}\mathbf{G}\right)^k \mathbf{S}^{-1}, \tag{19}$$

where $\mathbf{X}$ is replaced with the stair matrix $\mathbf{S}$ and the Gram matrix is considered. The convergence condition for Equation (19) is

$$\lim_{k \to \infty} \left(\mathbf{I} - \mathbf{S}^{-1}\mathbf{G}\right)^k = \mathbf{0}, \tag{20}$$

or equivalently

$$\rho\left(\mathbf{I} - \mathbf{S}^{-1}\mathbf{G}\right) = \lambda_0 < 1, \tag{21}$$

where $\rho(\mathbf{A})$ is the spectral radius of the matrix $\mathbf{A}$, and $|\lambda_0| \geqslant |\lambda_1| \geqslant \cdots \geqslant |\lambda_{N_U}|$ denote the N_U eigenvalues.

The convergence condition is critical for the application of the stair matrix in massive MIMO systems. In order to investigate the spectral radium of $\mathbf{I} - \mathbf{S}^{-1}\mathbf{G}$, we suppose N_U is odd [2], and define $\mathbf{B} = \mathbf{I} - \mathbf{S}^{-1}\mathbf{G}$, with each entry given by Equation (22), where **Algorithm 1** is used to compute the matrix inverse of the stair matrix.

We have the following Lemmas:

Lemma 1: $\mathbf{B}_{(u,v)}$ is given by Equation (22). For $u \in \mathbb{U}_1, v \neq u$ and $N_B > 4$, we have

$$\mathrm{E}\left\{\left|\mathbf{B}_{(u,v)}\right|^2\right\} \leqslant \sqrt{\frac{A_1}{B_1}}, \tag{23}$$

where A_1 and B_1 are respectively given by

$$A_1 = 2N_B\left(N_B+1\right), \tag{24}$$

$$B_1 = \left(N_B-1\right)\left(N_B-2\right)\left(N_B-3\right)\left(N_B-4\right). \tag{25}$$

Proof: See Appendix B. ■

Lemma 2: $\mathbf{B}_{(u,v)}$ is given by Equation (22). For $u \in \mathbb{U}_2$, $v \in \{u-1, u+1\}$, and $N_B > 4$, we have

$$\mathrm{E}\left\{\left|\mathbf{B}_{(u,v)}\right|^2\right\} \leqslant \frac{\sqrt{A_2}}{B_1}, \tag{26}$$

where B_1 is given by Equation (25), and A_2 is given by

$$\begin{aligned} A_2 = {} & 96N_B + 4N_B\left(N_B-1\right)\left(N_B-2\right)\left(N_B-3\right) \\ & + 144N_B\left(N_B-1\right) + 48N_B\left(N_B-1\right)\left(N_B-2\right), \end{aligned} \tag{27}$$

[1]For illustration consideration, we investigate the stair matrix in linear ZF detection. However, similar analysis for the stair matrix in linear MMSE detection is straightforward by following the similar process, and the applicability can be demonstrated as well.

[2]When N_U is even, the difference in the expression of $\mathbf{B}$ is only present in the last row. However, the general result is also expected.

Proof: See Appendix C. ■

Lemma 3: $\mathbf{B}_{(u,v)}$ is given by Equation (22). For $u \in \mathbb{U}_2$, $v \notin \{u-1, u, u+1\}$, and $N_B > 4$, we have

$$\mathrm{E}\left\{\left|\mathbf{B}_{(u,v)}\right|^2\right\} \leqslant \sqrt{\frac{12A_2A_3 + 6A_1A_3^2 + 24A_4 + 48\sqrt{A_1A_2A_3^3}}{B_1^3}} \tag{28}$$

where A_1, A_2, and B_1 are given by Equations (24), (27), and (25), respectively. A_3 and A_4 are respectively given by

$$\begin{aligned} A_3 = {} & 24N_B + N_B\left(N_B-1\right)\left(N_B-2\right)\left(N_B-3\right) \\ & + 36N_B\left(N_B-1\right) + 12N_B\left(N_B-1\right)\left(N_B-2\right), \end{aligned} \tag{29}$$

$$\begin{aligned} A_4 = {} & N_B\left(N_B-1\right)\left(N_B-2\right)^3\left(N_B-3\right)^3 \\ & + 26N_B\left(N_B-1\right)\left(N_B-2\right)^3\left(N_B-3\right)^2 \\ & + 46N_B\left(N_B-1\right)\left(N_B-2\right)^2\left(N_B-3\right)^2 \\ & + 4N_B\left(N_B-1\right)^2\left(N_B-2\right)^3\left(N_B-3\right) \\ & + 220N_B\left(N_B-1\right)\left(N_B-2\right)^3\left(N_B-3\right) \\ & + 48N_B\left(N_B-1\right)^2\left(N_B-2\right)^2\left(N_B-3\right) \\ & + 808N_B\left(N_B-1\right)\left(N_B-2\right)^2\left(N_B-3\right) \\ & + 128N_B\left(N-1\right)^2\left(N_B-2\right)\left(N_B-3\right) \\ & + 832N_B\left(N_B-1\right)\left(N_B-2\right)\left(N_B-3\right) \\ & + 40N_B\left(N_B-1\right)^2\left(N_B-2\right)^3 \\ & + 600N_B\left(N_B-1\right)\left(N_B-2\right)^3 \\ & + 4N_B\left(N_B-1\right)^3\left(N_B-2\right)^2 \\ & + 576N_B\left(N_B-1\right)^2\left(N_B-2\right)^2 \\ & + 3480N_B\left(N_B-1\right)\left(N_B-2\right)^2 \\ & + 64N_B\left(N_B-1\right)^3\left(N_B-2\right) \\ & + 2592N_B\left(N_B-1\right)^2\left(N_B-2\right) \\ & + 8064N_B\left(N_B-1\right)\left(N_B-2\right) \\ & + 256N_B\left(N_B-1\right)^3 \\ & + 4352N_B\left(N_B-1\right)^2 \\ & + 9888N_B\left(N_B-1\right) \\ & + 2304N_B. \end{aligned} \tag{30}$$

Proof: See Appendix D. ■

Lemma 4: $\mathbf{B}_{(u,v)}$ is given by Equation (22). For $u \in \mathbb{U}_2$, $v = u$, and $N_B > 4$, we have

$$\mathrm{E}\left\{\left|\mathbf{B}_{(u,u)}\right|^2\right\} \leqslant \sqrt{\frac{16A_3A_5}{B_1^3}}, \tag{31}$$

where A_3 and B_1 are given by Equations (29) and (25), respectively. A_5 is given by

$$\begin{aligned} A_5 = {} & 576N_B + 24N_B\left(N_B-1\right)\left(N_B-2\right)\left(N_B-3\right) \\ & + 864N_B\left(N_B-1\right) + 288N_B\left(N_B-1\right)\left(N_B-2\right). \end{aligned} \tag{32}$$

Proof: See Appendix E. ■

With the results in ***Lemma 1* - *4***, we have

$$\begin{aligned}\mathrm{E}\left\{\|\mathbf{B}\|_{\mathrm{F}}^{2}\right\} &= \sum_{u=1}^{N_U}\sum_{v=1}^{N_U}\mathrm{E}\left\{\left|\mathbf{B}_{(u,v)}\right|^{2}\right\}\\ &\leqslant \frac{N_U^2-1}{2}\sqrt{\frac{A_1}{B_1}}+(N_U-1)\frac{\sqrt{A_2}}{B_1}+\frac{(N_U-1)}{2}\sqrt{\frac{16A_3A_5}{B_1^3}}\\ &+\frac{N_U^2-4N_U+3}{2}\sqrt{\frac{12A_2A_3+6A_1A_3^2+24A_4+48\sqrt{A_1A_2A_3^3}}{B_1^3}}\end{aligned} \tag{33}$$

Apparently, at the right hand side of the inequality (33), as the power in numerator is much less than that in denominator, we can derive

$$\lim_{N_B\to\infty}\mathrm{E}\left\{\|\mathbf{B}\|_{\mathrm{F}}^{2}\right\}=0. \tag{34}$$

Applying the Markov's inequality, we have

$$\Pr\left\{\|\mathbf{B}\|_{\mathrm{F}}^{2}<1\right\}=1-\Pr\left\{\|\mathbf{B}\|_{\mathrm{F}}^{2}\geqslant 1\right\}\geqslant 1-\mathrm{E}\left\{\|\mathbf{B}\|_{\mathrm{F}}^{2}\right\}. \tag{35}$$

As $\|\mathbf{B}\|_{\mathrm{F}}^{2}=\sum_{i=0}^{N_U-1}|\lambda_i|^2$, together with the inequality (35), we can see that with sufficiently large number of antennas at base station (i.e., $N_B\to\infty$), the probability that convergence condition in (21) is satisfied, will approach 1.

Following the similar analysis, we can also demonstrated that with sufficient large N_B, using stair matrix, the probability that the convergence condition is met will also approach 1 in the approximation of the linear MMSE estimation.

Hence we demonstrate the applicability of the stair matrix in massive MIMO systems.

C. Residual Estimation Error

We now investigate the residual estimation error by using the truncated Neumann series expansion. According to Equation (12), we have

$$\mathbf{G}_L^{-1}=\sum_{l=0}^{L-1}\left(\mathbf{S}^{-1}(\mathbf{S}-\mathbf{G})\right)^{l}\mathbf{S}^{-1}. \tag{36}$$

Replacing $\mathbf{G}^{-1}$ with $\mathbf{G}_L^{-1}$ in Equation (4), we have

$$\hat{\mathbf{x}}^{(L)}=\mathbf{G}_L^{-1}\mathbf{y}^{\mathrm{MF}}. \tag{37}$$

Therefore, the residual estimation error $J=\left\|\hat{\mathbf{x}}^{(L)}-\hat{\mathbf{x}}\right\|_2$, is bounded as

$$\begin{aligned}J &= \left\|\left(\mathbf{G}^{-1}-\mathbf{G}_L^{-1}\right)\mathbf{y}^{\mathrm{MF}}\right\|_2\\ &= \left\|\sum_{l=L}^{\infty}\left(\mathbf{S}^{-1}(\mathbf{S}-\mathbf{G})\right)^{l}\mathbf{S}^{-1}\mathbf{y}^{\mathrm{MF}}\right\|_2\\ &= \left\|\left(\mathbf{S}^{-1}(\mathbf{S}-\mathbf{G})\right)^{L}\mathbf{G}^{-1}\mathbf{y}^{\mathrm{MF}}\right\|_2\\ &\leqslant \|\mathbf{B}\|_{\mathrm{F}}^{L}\|\hat{\mathbf{x}}\|_2,\end{aligned} \tag{38}$$

where the inequality holds since $\|\mathbf{A}\mathbf{x}\|_2\leqslant\|\mathbf{A}\|_{\mathrm{F}}\|\mathbf{x}\|_2$. As $N_B\to\infty$, $\Pr\left\{\|\mathbf{B}\|_{\mathrm{F}}^{2}<1\right\}\to 1$. That is to say, the residual estimation error will approach 0 as indicated by inequality (38). Inequality (38) also indicates that increasing the truncation order in Neumann series expansion, the upper bound of the residual estimation error can be reduced. This evidence, together with high probability with the convergence condition to be met, supports the applications of the stair matrix to massive MIMO systems.

IV. Implementation of the Stair Matrix in Iterative Method

Due to the involvement of matrix multiplications, the truncation order in Neumann series expansion is limited to three; otherwise, the computational complexity is comparable with matrix inversion algorithm. Besides, we note that in existing work, the computation of the LLR is obtained by utilizing the NPI after the first truncation order in Neumann series expansion (or first iteration in iterative method). This implementation, however, causes significant performance loss when N_B is not sufficiently large (or $r=N_B/N_U$ is not large, for example, $r<8$). In this section, we address these issues in the application of stair matrix in iterative method.

A. Stair Matrix in Iterative Method

Compared to the linear ZF detection, linear MMSE detection achieves a better balance in consideration of interference and noise. Therefore, we will introduce an iterative method to approach the linear MMSE detection.

To start with, we define the stair matrix $\mathbf{S}=\mathrm{stair}\left(\mathbf{W}_{(u,u-1)},\mathbf{W}_{(u,u)},\mathbf{W}_{(u,u+1)}\right)$. It is worth noting that compared to the stair matrix we discussed in previous section, the diagonal elements in the new stair matrix has increased by σ_z^2 according to Equation (3), which brings negligible computational cost. According to Equation (17), we have

$$\begin{aligned}\mathbf{x}^{(i+1)} &= \mathbf{S}^{-1}\left((\mathbf{S}-\mathbf{W})\mathbf{x}^{(i)}+\mathbf{y}^{\mathrm{MF}}\right)\\ &= \mathbf{x}^{(i)}-\mathbf{S}^{-1}\mathbf{W}\mathbf{x}^{(i)}+\mathbf{S}^{-1}\mathbf{y}^{\mathrm{MF}},\end{aligned} \tag{39}$$

where $\mathbf{x}^{(i)}$ is the i-th estimation.

In accordance, if the initial estimation $\mathbf{x}^{(0)}$ is selected as

$$\mathbf{x}^{(0)}=\mathbf{S}^{-1}\mathbf{y}^{\mathrm{MF}}, \tag{40}$$

following the iterative process in Equation (39), we can derive

$$\mathbf{x}^{(i)}=\sum_{l=0}^{i}\left(\mathbf{S}^{-1}(\mathbf{S}-\mathbf{W})\right)^{l}\mathbf{S}^{-1}\mathbf{y}^{\mathrm{MF}}, \tag{41}$$

which indicates that the iterative method in Equation (39) can be seen as truncated Neumann series expansion method. However, in Equation (39), only matrix-vector product is involved, hence the overall computational complexity is of the order $\mathcal{O}\left(KN_U^2\right)$, where K denotes the iteration numbers.

B. Computation of the LLR

After the estimation of transmitted vector $\mathbf{x}$, we need to compute the LLRs of the associated bits for the soft-input channel decoder. After K iterations, the equivalent channel gain $\rho_u^{(K)}$ and the covariance of the NPI $\left|v_u^{(K)}\right|^2$ can be respectively given by

$$\rho_u^{(K)}=\mathbf{e}_u^{\mathrm{H}}\mathbf{W}_K^{-1}\mathbf{G}\mathbf{e}_u, \tag{42}$$

$$\left|v_u^{(K)}\right|^2=\mathbf{e}_u^{\mathrm{H}}\mathbf{W}_K^{-1}\mathbf{G}\mathbf{G}\mathbf{W}_K^{-1}\mathbf{e}_u+\sigma_z^2\mathbf{e}_u^{\mathrm{H}}\mathbf{W}_K^{-1}\mathbf{G}\mathbf{W}_K^{-1}\mathbf{e}_u-\left|\rho_u^{(K)}\right|^2 \tag{43}$$

Apparently, Equations (42) and (43) requires matrix multiplications if $K \geq 2$. Therefore, in [8], [13]–[15], $\mathbf{D}^{-1}$, which is the first truncation order, is considered for the simplification. This approximation, however, as we will show in the next section, has caused a significant performance loss.

As we can see from Equation (8), the exact *a posteriori* covariance of the NPI in linear MMSE estimation can be derived if the equivalent channel gain is obtained. However, in [8], the authors have claimed that this relationship is not supported in truncated Neumann series expansion. The main reason for that claim is attributed to the fact that $\mathbf{W}_K^{-1}$ is far away from $\mathbf{W}^{-1}$ with small K. In previous section, we introduce the iterative method for detection, and the iteration numbers can be sufficiently large since the computational complexity in one iteration is of the order $\mathcal{O}\left(N_U^2\right)$. With sufficiently large iterations, $\mathbf{W}_K^{-1}$ can be quite close to $\mathbf{W}^{-1}$ (we will show this in the next section); hence, we can used Equation (8) to derive the covariance of the NPI. The next question is how to maintain low computational complexity to obtain the equivalent channel gain.

We rewrite the equivalent channel gain in Equation (8) as $\rho_u = \mathbf{e}_u^{\mathrm{H}}\mathbf{W}^{-1}\mathbf{G}\mathbf{e}_u = 1 - \sigma_z^2\mathbf{e}_u^{\mathrm{H}}\mathbf{W}^{-1}\mathbf{e}_u$. In addition, we replace $\mathbf{W}^{-1}$ with $\mathbf{W}_K^{-1}$, leading to

$$\rho_u^{(K)} = 1 - \sigma_z^2\mathbf{e}_u^{\mathrm{H}}\mathbf{W}_K^{-1}\mathbf{e}_u. \tag{44}$$

That is to say, we need obtain the diagonal elements in $\mathbf{W}_K^{-1}$ to compute $\rho_u^{(K)}$.

If N_B and r are sufficiently large, the Gram matrix $\mathbf{G}$ and $\mathbf{W}$ will become diagonal dominant; therefore, $\mathbf{D}^{-1}$ can be a good approximation of $\mathbf{W}^{-1}$, and we have the approximation to $\rho_u^{(K)}$ given by

$$\rho_u^{(K)} \approx 1 - \sigma_z^2\mathbf{D}_{(u,u)}^{-1}, \tag{45}$$

and $\left|v_u^{(K)}\right|^2$ is approximated as

$$\left|v_u^{(K)}\right|^2 \approx \rho_u^{(K)}\left(1 - \rho_u^{(K)}\right). \tag{46}$$

As a consequence, the *a posteriori* SINR is approximated as

$$\gamma_u^{(K)} \approx \frac{\left|\rho_u^{(K)}\right|^2}{\left|v_u^{(K)}\right|^2} = \frac{\rho_u^{(K)}}{1 - \rho_u^{(K)}}. \tag{47}$$

$\rho_u^{(K)}$ and $\gamma_u^{(K)}$ are used in Equation (9) to compute $L\left(b_{u,k}\right)$.

It is worth pointing out that although we utilize the diagonal matrix to estimate the equivalent channel gain, the computation of $\gamma_u^{(K)}$ in Equation (47) indicates that we try to approach the SINR in linear MMSE detection to derive the LLRs of the associated bits. This is quite different from the existing work [8], [13]–[15], where the SINR after the first iteration (or the first truncation order in Neumann series expansion method) is adopted. In fact, as the iterations increase, the covariance of the NPI will decrease, and our proposed approximation method is more efficient and accurate. In numerical simulations, we also validate that our approximation in (45) and (47) outperforms the approximation in existing work.

To summarize, we present **Algorithm 2** for the proposed iterative method using stair matrix.

Algorithm 2: Proposed Iterative Method Using Stair Matrix

Input: $\mathbf{y}$, $\mathbf{H}$, σ_z^2, and Iteration number K;

Output: LLRs of the associated bits $L\left(b_{u,k}\right)$.

Initialization:

1.$\mathbf{G} = \mathbf{H}^{\mathrm{H}}\mathbf{H}$, $\mathbf{W} = \mathbf{G} + \sigma_z^2\mathbf{I}_{N_U}$, $\mathbf{y}^{\mathrm{MF}} = \mathbf{H}^{\mathrm{H}}\mathbf{y}$;

2. $\mathbf{S} = \mathrm{stair}\left(\mathbf{W}_{(u,u-1)}, \mathbf{W}_{(u,u)}, \mathbf{W}_{(u,u+1)}\right)$;

3. Compute $\mathbf{S}^{-1}$ through **Algorithm 1**, and $\mathbf{D}^{-1} = \mathrm{diag}\left(\mathbf{S}^{-1}\right)$;

4. Initial estimation: $\mathbf{x}^{(0)} = \mathbf{S}^{-1}\mathbf{y}^{\mathrm{MF}}$;

Iteration:

5. for $i = 1 : 1 : K$

6. $\quad \mathbf{x}^{(i+1)} = \mathbf{S}^{-1}\left(\left(\mathbf{S} - \mathbf{W}\right)\mathbf{x}^{(i)} + \mathbf{y}^{\mathrm{MF}}\right)$;

7. end

LLR Computation:

8. $\rho_u^{(K)} = 1 - \sigma_z^2\mathbf{D}_{(u,u)}^{-1}$, $\gamma_u^{(K)} = \frac{\rho_u^{(K)}}{1-\rho_u^{(K)}}$;

9. $L\left(b_{u,k}\right) = \gamma_u^{(K)}\left(\min_{s\in\chi_k^0}\left|\frac{\hat{x}_u^{(K)}}{\rho_u^{(K)}} - s\right|^2 - \min_{s'\in\chi_k^1}\left|\frac{\hat{x}_u^{(K)}}{\rho_u^{(K)}} - s'\right|^2\right)$.

Return $L\left(b_{u,k}\right)$.

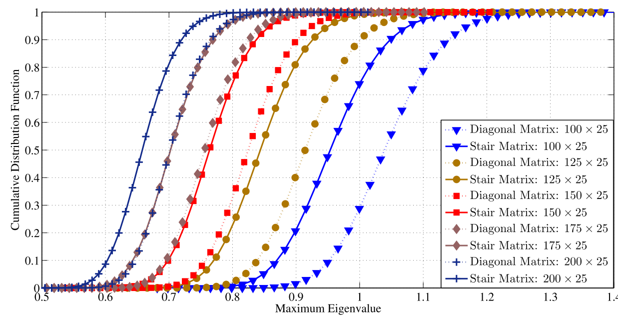

Fig. 1. Cumulative distribution function of the maximum eigenvalue $N_U = 25$.

C. Computational Complexity Analysis

We consider the number of real number multiplications/divisions to evaluate the computational complexity. In initialization steps, the computation of $\mathbf{W}$ and $\mathbf{y}^{\mathrm{MF}}$ requires $2N_BN_U^2$ and $4N_BN_U$ real number multiplications, respectively. According to **Algorithm 1**, the computation of $\mathbf{S}^{-1}$ requires $3\left(N_U - 1\right)$ real number multiplications and N_U real number divisions. The initial estimation, provided in Step 4, requires $\frac{N_U+1}{2} \times 2 + \frac{N_U-1}{2} \times (8+2) = 6N_U - 4$ real number multiplications. Therefore, the total computational complexity in initialization steps is $2N_BN_U^2 + 4N_BN_U + 10N_U - 7$.

The iteration steps in **Algorithm 2** involves matrix-vector production. The computation of $\left(\mathbf{S} - \mathbf{W}\right)\mathbf{x}^{(i)}$ requires $\frac{N_U+1}{2} \times 4\left(N_U - 1\right) + \frac{N_U-1}{2} \times 4\left(N_U - 3\right) = 4(N_U - 1)^2$ real number multiplications. The resultant vector is multiplied by a stair matrix, and additional $6N_U - 4$ real number multiplications are required. Therefore, the total computational complexity in iteration steps is $K\left(4N_U^2 - 2N_U\right)$. That is to say, the computational complexity of the iterative process is of $\mathcal{O}\left(N_U^2\right)$, which is the same as the existing iterative methods where the diagonal matrix is applied.

Last, to obtain $L\left(b_{k,u}\right)$, we need the computation of $\rho_u^{(K)}$, and the proposed approximation method only requires the diagonal elements in $\mathbf{D}$, which is obtained in step 3. Compared to the existing work in [8], [13]–[15], our proposed scheme saves computational complexity in this stage.

To summarize, the overall computational complexity is the same level of the existing work. However, as we will see in next section, the stair matrix outperforms the diagonal matrix at all round.

V. Numerical Simulations and Performance Evaluation

A. Convergence Conditions

We first investigate the convergence condition using the stair matrix. Using Monte-Carlo method, we generate 2e7 random channel matrix $\mathbf{H}$. For each $\mathbf{H}$, we extract the diagonal matrix $\mathbf{D}$ and the stair matrix $\mathbf{S}$, and compute the maximum eigenvalues of the matrix $\mathbf{I}-\mathbf{D}^{-1}\mathbf{G}$, and $\mathbf{I}-\mathbf{S}^{-1}\mathbf{G}$, respectively. Using numerical simulations, we eventually obtain the cumulative distribution function (CDF) of the maximum eigenvalues, given by Figure 1. In Figure 1, we evaluate the scenario that 25 users are in service and we increase the number of antennas at base station from 100 to 200. The following observations can be found:

- With the increase of antennas at base station, the probability that the convergence conditions are met, i.e., $\Pr\left\{\rho\left(\mathbf{I}-\mathbf{S}^{-1}\mathbf{G}\right)<1\right\}$ and $\Pr\left\{\rho\left(\mathbf{I}-\mathbf{D}^{-1}\mathbf{G}\right)<1\right\}$ will increase. Specifically, for the usage of the diagonal matrix, the probability that the convergence conditions are met, is increase from 0.29 when $N_B=100$, to 1 when $N_B=200$. In accordance, for the usage of the stair matrix, $\Pr\left\{\rho\left(\mathbf{I}-\mathbf{S}^{-1}\mathbf{G}\right)<1\right\}$ is increased from 0.74 when $N_B=100$, to 1 when $N_B=200$;
- In low $r=N_B/N_U\leq 5$ region, the usage of the stair matrix can increase the probability that the convergence conditions are met. For example, when $N_B=100$, $\Pr\left\{\rho\left(\mathbf{I}-\mathbf{D}^{-1}\mathbf{G}\right)<1\right\}$ is only 0.29, while $\Pr\left\{\rho\left(\mathbf{I}-\mathbf{S}^{-1}\mathbf{G}\right)<1\right\}$ becomes 0.76. This indicates that in some low r region, the diagonal matrix is not applicable while the stair matrix can be used;
- In any system configuration, $\Pr\left\{\rho\left(\mathbf{I}-\mathbf{S}^{-1}\mathbf{G}\right)<a\right\}\geqslant\Pr\left\{\rho\left(\mathbf{I}-\mathbf{D}^{-1}\mathbf{G}\right)<a\right\}$, $a\in(0,1)$. As the maximum eigenvalue determines the convergence rate, we can conclude that by using the stair matrix, the convergence rate is more likely faster compare to the usage of the diagonal matrix.

The above observations validate the applicability of the usage of the stair matrix and diagonal matrix in massive MIMO systems. Besides, the results reveal that by using stair matrix, we can increase the probability that the convergence conditions are met in low r region compared to the usage of the diagonal matrix. Furthermore, we also find that by using the stair matrix, the convergence rate is more likely accelerated than the usage of the stair matrix.

B. Matrix Inverse

we now investigate the performance of the stair matrix in Neumann series expansion to approach the matrix inverse[3]. We define $\mathbf{\Delta}(\mathbf{S})=\frac{1}{N_U}\left(\mathbf{I}-\sum_{l=0}^{L-1}\left(\mathbf{I}-\mathbf{S}^{-1}\mathbf{G}\right)^l\mathbf{S}^{-1}\mathbf{G}\right)$

[3]In implementation, we propose the iterative method as shown in section IV. However, the results of the iterative method can be seen as the Neumann series expansion.

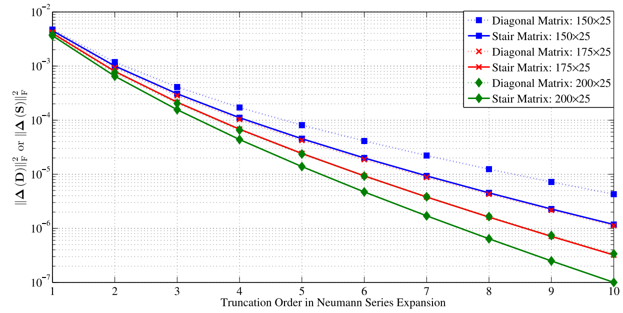

Fig. 2. Normalized mean-square error for the matrix inverse approximation

where $\mathbf{S}=\mathrm{stair}\left(\mathbf{G}_{u,u-1},\mathbf{G}_{u,u},\mathbf{G}_{u,u+1}\right)$, and $\mathbf{\Delta}(\mathbf{D})=\frac{1}{N_U}\left(\mathbf{I}-\sum_{l=0}^{L-1}\left(\mathbf{I}-\mathbf{D}^{-1}\mathbf{G}\right)^l\mathbf{D}^{-1}\mathbf{G}\right)$ where $\mathbf{D}=\mathrm{diag}(\mathbf{G})$. In addition, we have $\|\mathbf{\Delta}(\mathbf{S})\|_F^2$ and $\|\mathbf{\Delta}(\mathbf{D})\|_F^2$ to indicate the normalized mean-square error for the approximation using the stair matrix and the diagonal matrix, respectively. With different truncation order, we present the results in Figure 2. The following observations can be found:

- With the increase of the truncation order, the normalized mean-square error is decreased. This indicates that the more truncation orders used in Neumann series expansion, the more close of the resulting approximation of the matrix inverse is obtained;
- By using the stair matrix, the normalized mean-square error is always less than that of using the diagonal matrix in the same system configuration. This indicates that the use of the stair matrix always achieves better approximation performance with the same truncation order compared to the use of the diagonal matrix;
- By using the stair matrix, less iterations are required to achieve the the same level of the normalized mean-square error in using the diagonal matrix. As the truncation order is equivalent to the iteration number in iterative method, the less iterations indicate less computational complexity in implementation.

To summarize, we conclude that the usage of the stair matrix outperforms the usage of the diagonal matrix in terms of the matrix inverse approximation performance. As we showed in section IV.A, the truncation order is equivalent to the iterations in iterative method; therefore, the results in Figure 2 help to interpret the convergence performance of the iterative method.

C. Residual Estimation Error

In iterative method, the estimation is to approach the estimation vector in linear ZF/MMSE method. In section IV.C, an upper bound of the residual estimation error for the use of the stair matrix in approaching linear ZF detection is presented. In order to differentiate the residual estimation error for the use of stair matrix and the diagonal matrix in linear ZF and

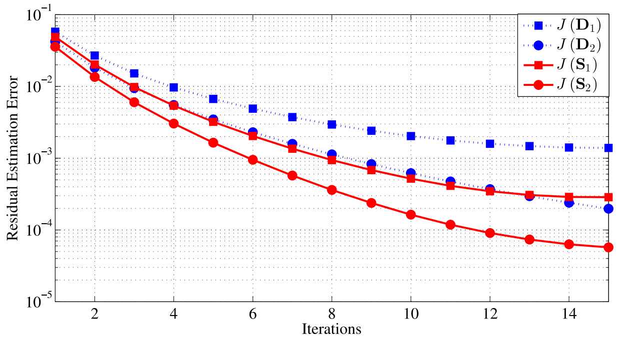

(a)

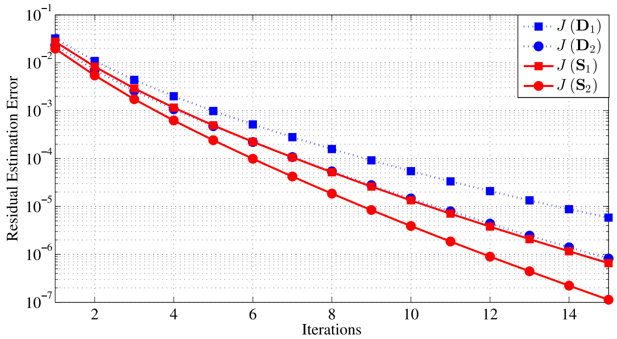

(b)

Fig. 3. Residual Estimation Error: (a) N_B = 150, N_U = 25, average SNR= 5dB; (b) N_B = 200, N_U = 25, average SNR= 3.5dB

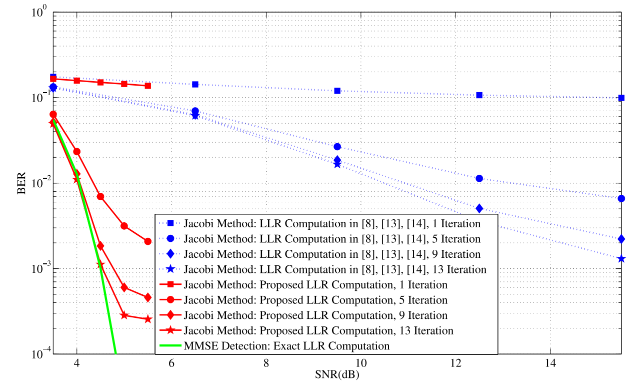

(a)

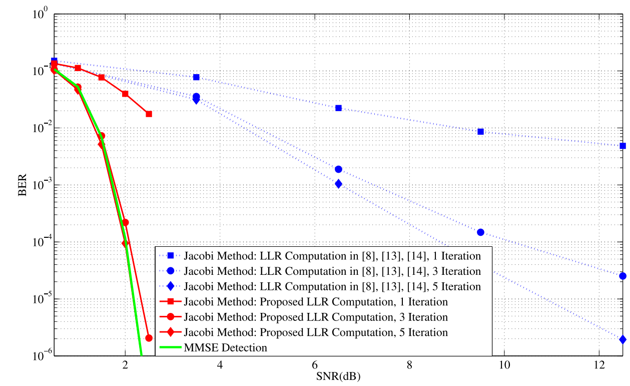

(b)

Fig. 4. BER performance: (a) N_B = 150, N_U = 25; (b) N_B = 250, N_U = 25.

MMSE detection, we define the following terms:

$$J(\mathbf{D}_1) = \left\| \left(\mathbf{D}_1^{-1}(\mathbf{D}_1 - \mathbf{G})\right)^L \mathbf{G}^{-1}\mathbf{y}^{\mathrm{MF}} \right\|_2,$$
$$J(\mathbf{D}_2) = \left\| \left(\mathbf{D}_2^{-1}(\mathbf{D}_2 - \mathbf{W})\right)^L \mathbf{W}^{-1}\mathbf{y}^{\mathrm{MF}} \right\|_2,$$
$$J(\mathbf{S}_1) = \left\| \left(\mathbf{S}_1^{-1}(\mathbf{S}_1 - \mathbf{G})\right)^L \mathbf{G}^{-1}\mathbf{y}^{\mathrm{MF}} \right\|_2,$$
$$J(\mathbf{S}_2) = \left\| \left(\mathbf{S}_2^{-1}(\mathbf{S}_2 - \mathbf{W})\right)^L \mathbf{W}^{-1}\mathbf{y}^{\mathrm{MF}} \right\|_2,$$

where $\mathbf{W} = \mathbf{G} + \sigma_z^2 \mathbf{I}_{N_U}$, $\mathbf{D}_1 = \mathrm{diag}\{\mathbf{G}\}$, $\mathbf{D}_2 = \mathrm{diag}\{\mathbf{W}\}$, $\mathbf{S}_1 = \mathrm{stair}(\mathbf{G}_{m,m-1}, \mathbf{G}_{m,m}, \mathbf{G}_{m,m+1})$, and $\mathbf{S}_2 = \mathrm{stair}(\mathbf{W}_{m,m-1}, \mathbf{W}_{m,m}, \mathbf{W}_{m,m+1})$. According to Equation (38), we can see that $J(\mathbf{D}_1)$ and $J(\mathbf{D}_2)$ denote the residual estimation error for the use of the diagonal matrix in approaching linear ZF and MMSE detection, respectively. $J(\mathbf{S}_1)$ and $J(\mathbf{S}_2)$ denote the residual estimation error for the use of the stair matrix in approaching linea ZF and MMSE detection, respectively. For a given system configuration and average receiving SNR, we present the residual estimation error performance in Figure 3. The following observations are found:

- From Figure 3(a) and 3(b), $J(\mathbf{S}_1)$ is always less than $J(\mathbf{D}_1)$, and $J(\mathbf{S}_2)$ is always less than $J(\mathbf{D}_2)$ after the same iteration numbers. These results reflect that after the same iterations, using the stair matrix in iterative method can approach both the linear ZF and MMSE estimation more closely compared to the use of the diagonal matrix;
- In Figure 3(a), we note that, for the use of the diagonal matrix, the residual estimation error decreases slowly and remains a comparatively high level even with large iteration numbers. However, by using the stair matrix, we can speed up the decreasing rate and achieve a comparatively lower estimation error level. These results are consistent with the previous numerical results where we demonstrate that the use of the diagonal matrix may not be applicable in low r ratio.
- From Figure 3(a) and Figure 3(b), we can see that, with the increase of the receiving antennas at base station, the performance gain of the use of the stair matrix over the use of the diagonal matrix becomes small. These results are reasonable as N_B increases large, $\mathbf{G}$ and $\mathbf{W}$ both become diagonal dominant. However, we can also achieve comparatively lower residual estimation error by using the stair matrix in iterative method.

To summarize, we conclude that the use of the stair matrix outperforms the use of the diagonal matrix in terms of the residual estimation error. The performance gain is more significant in low r ratio, but still obvious in high r ratio.

D. BER Performance

We now evaluate the system BER performance. In the system, the base station is simultaneously serving N_U = 25 users. For each user, a LDPC code with code length 64800, code rate 1/2 is considered for channel code scheme[4]. We con-

[4]LDPC code has been an agreed standard for long code in 5G

sider 64QAM modulation, and a block independent channel is considered for the evaluation.

To begin with, we investigate the proposed LLR computation given by (47), and the equivalent channel gain ρ_u and the covariance of the NPI v_u are approximated by (45) and (46). For comparison, we provide the linear MMSE detection as a benchmark, where the LLR computation is given by Equation (9) with ρ_u and v_u given by Equation (6) and (8), respectively. The LLR computation in existing work such as [8], [13], [14] is to compute the covariance of the NPI after the first iteration. It is worth pointing out that the iterative methods in [13], [14] requires less iterations to approach the linear MMSE detection; however, the LLR computation used in MMSE detection is not computed from the exact NPI of the MMSE detection, but the NPI after the first iteration. In Figure 4, we can see that the BER performance of the Jacobi method with the LLR computation in [8], [13], [14] is far away from the BER performance of the MMSE detection with the exact LLR computation. This is consistent with our previous analysis, where we pointed out that the covariance of the NPI will decrease with iterations. However, we note that the proposed LLR computation can greatly improve the BER performance of the Jacobi method by approximating the covariance of the NPI of the MMSE detection. Hereafter, we only utilize the proposed LLR computation for the BER performance comparison.

We now present the results with low $r = N_B/N_U$ region, and the results are presented in Figure 5. The following observations are found.

- From Figure 5(a), we note that the BER performance improvement with the proposed stair matrix compared to the diagonal matrix is obvious. However, the system performance is still far away from the MMSE detection even with sufficient large iterations. Specially, for the use of the diagonal matrix, the performance is level off after 9 iterations; for the use of the stair matrix, the performance is greatly improved, but a level off performance still appears. These are attributed to the slow convergence rate and not a 100 percent convergence conditions satisfied;
- From Figure 5(b) and Figure 5(c), we can see that the BER performance eventually converges to the performance of the MMSE detection. Specifically, in the system configuration $N_B = 150$, $N_U = 25$, at SNR= $5dB$, the BER performance of the proposed iterative method after 13 iterations is almost the same as the performance of the MMSE detection. In the system configuration $N_B = 175$, $N_U = 25$, at SNR= $4dB$, the BER performance of the Jacobi method after 9 iterations approaches the performance of the MMSE detection;
- From Figure 5(a) to Figure 5(c), we can see that the convergence rate of the proposed iterative method is faster than that of the Jacobi method. These results are consistent with the previous analysis. With faster convergence rate, fewer iterations are required for the proposed iterative method, hence reducing the overall system computational complexity.

Next, we evaluate the BER performance in the system

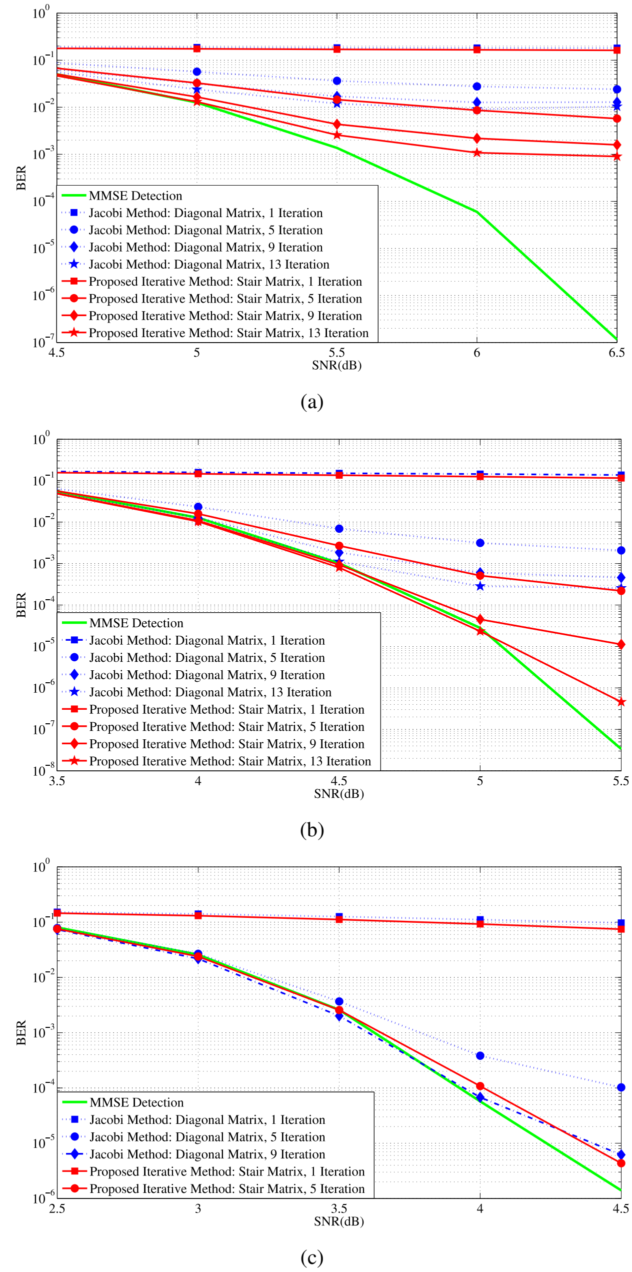

Fig. 5. BER performance: (a) N_B = 125, N_U = 25; (b) N_B = 150, N_U = 25; (c) N_B = 175, N_U = 25.

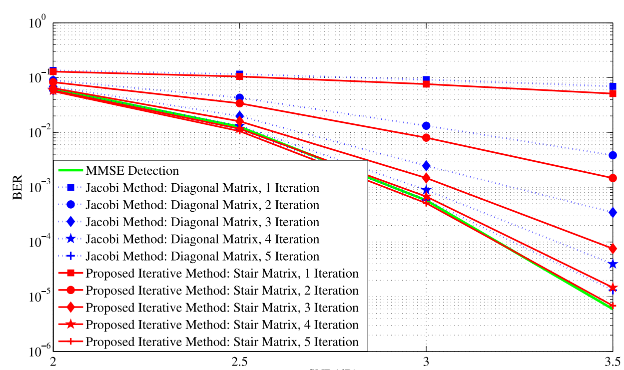

Fig. 6. BER performance: N_B = 200, N_U = 25.

configuration with high $r = N_B/N_U$ region, and the results are shown in Figure 6. It is clear that both the uses of the diagonal matrix and stair matrix require few iterations to converge. However, as indicated by the cumulative distribution function of the maximum eigenvalue, $\Pr\left\{\rho\left(\mathbf{I}-\mathbf{S}^{-1}\mathbf{G}\right)<a\right\} \geqslant \Pr\left\{\rho\left(\mathbf{I}-\mathbf{D}^{-1}\mathbf{G}\right)<a\right\}$, $a \in (0,1)$, we can conclude that the convergence rate of the proposed iterative method using the stair matrix is faster than that of the Jacobi method using the diagonal matrix. The results validate these conclusions.

VI. Conclusions

In this paper, we propose the application of the stair matrix in massive MIMO systems. To begin with, we demonstrate that with sufficient large number of antennas at base station, the probability that the convergence conditions are met with the use of the stair matrix approaches 1. We then propose an iterative method to reduce the computational complexity and show that the overall computational complexity is of the same level as the existing iterative methods where the diagonal matrix is applied. Furthermore, we evaluate the performance of the stair matrix in terms of the probability that the convergence conditions are met, the normalized mean-square error of in Neumann series expansion to approach the matrix inverse, the residual estimation error of the iterative method to approach the linear ZF/MMSE estimation, and the system BER performance. Numerical simulations show that performance enhancement by using the stair matrix over the diagonal matrix is presented in all performance metrics.

Appendix

A. Preliminaries

We first present the preliminary lemmas.

***Lemma** 5:* Let $a_k \sim CN(0,1)$, we then have

$$\mathrm{E}\left\{\left|a_k\right|^2\right\} = 1, \tag{48}$$

$$\mathrm{E}\left\{\left|a_k\right|^4\right\} = 2, \tag{49}$$

$$\mathrm{E}\left\{\left|a_k\right|^6\right\} = 6, \tag{50}$$

$$\mathrm{E}\left\{\left|a_k\right|^8\right\} = 24, \tag{51}$$

***Lemma** 6:* Let $\mathbf{a} = \left[a_1, a_2, \cdots, a_{N_B}\right]^{\mathrm{T}}$ with each entry $a_k \sim CN(0,1)$, independent and identically distributed (i.i.d.). We then have

$$\mathrm{E}\left\{\mathbf{a}^{\mathrm{H}}\mathbf{a}\right\} = N_B, \tag{52}$$

$$\mathrm{E}\left\{\left|\mathbf{a}^{\mathrm{H}}\mathbf{a}\right|^4\right\} = A_3, \tag{53}$$

$$\mathrm{E}\left\{\left|\mathbf{a}^{\mathrm{H}}\mathbf{a}\right|^{-4}\right\} = \frac{1}{B_1}, \tag{54}$$

where A_3 and B_1 are given by Equations (29) and (25).

***Lemma** 7:* Let $\mathbf{a} = \left[a_1, a_2, \cdots, a_{N_B}\right]^{\mathrm{T}}$, $\mathbf{b} = \left[b_1, b_2, \cdots, b_{N_B}\right]^{\mathrm{T}}$, with each entry $a_k \sim CN(0,1)$, $b_k \sim CN(0,1)$, and i.i.d., we then have

$$\mathrm{E}\left\{\left|\mathbf{a}^{\mathrm{H}}\mathbf{b}\right|^4\right\} = A_1, \tag{55}$$

$$\mathrm{E}\left\{\left|\mathbf{a}^{\mathrm{H}}\mathbf{b}\right|^8\right\} = A_5. \tag{56}$$

where A_1 and A_5 are given by Equations (24) and (32).

***Lemma** 8:* Let $A = \mathbf{a}^{\mathrm{H}}\mathbf{b}\mathbf{b}^{\mathrm{H}}\mathbf{c}$, where $\mathbf{a} = \left[a_1, a_2, \cdots, a_{N_B}\right]^{\mathrm{T}}$, $\mathbf{b} = \left[b_1, b_2, \cdots, b_{N_B}\right]^{\mathrm{T}}$, and $\mathbf{c} = \left[c_1, c_2, \cdots, c_{N_B}\right]^{\mathrm{T}}$, with each entry $a_k \sim CN(0,1)$, $b_k \sim CN(0,1)$, and $c_k \sim CN(0,1)$, and i.i.d., we then have

$$\mathrm{E}\left\{|A|^4\right\} = A_2, \tag{57}$$

where A_2 is given by Equation (27)

***Lemma** 9:* Let $A = \mathbf{a}^{\mathrm{H}}\mathbf{a}\mathbf{b}^{\mathrm{H}}\mathbf{b}\mathbf{c}^{\mathrm{H}}\mathbf{b}\mathbf{b}^{\mathrm{H}}\mathbf{d}\mathbf{a}^{\mathrm{H}}\mathbf{c}\mathbf{d}^{\mathrm{H}}\mathbf{a}$, where $\mathbf{a} = \left[a_1, a_2, \cdots, a_{N_B}\right]^{\mathrm{T}}$, $\mathbf{b} = \left[b_1, b_2, \cdots, b_{N_B}\right]^{\mathrm{T}}$, $\mathbf{c} = \left[c_1, c_2, \cdots, c_{N_B}\right]^{\mathrm{T}}$, and $\mathbf{d} = \left[d_1, d_2, \cdots, d_{N_B}\right]^{\mathrm{T}}$, with each entry $a_k \sim CN(0,1)$, $b_k \sim CN(0,1)$, $c_k \sim CN(0,1)$, and $d_k \sim CN(0,1)$, and i.i.d., we then have

$$E\left\{A^2\right\} = A_4, \tag{58}$$

where A_4 is given by Equation (30).

B. Proof of ***Lemma 1***

For $u \in \mathbb{U}_1, v \neq u$, from Equation (22), we have

$$\begin{aligned}\mathrm{E}\left\{\left|\mathbf{B}_{(u,v)}\right|^2\right\} &= \mathrm{E}\left\{\frac{\left|\mathbf{W}_{(u,v)}\right|^2}{\left|\mathbf{W}_{(u,u)}\right|^2}\right\} \\ &\leqslant \sqrt{\mathrm{E}\left\{\left|\mathbf{W}_{(u,v)}\right|^4\right\}\cdot\mathrm{E}\left\{\left|\mathbf{W}_{(u,u)}\right|^{-4}\right\}},\end{aligned} \tag{59}$$

where the Cauchy-Schwarz inequality is applied [8]. From ***Lemma 7*** and ***Lemma 6***, we have

$$\mathrm{E}\left\{\left|\mathbf{W}_{u,v}\right|^4\right\} = A_1, \tag{60}$$

$$\mathrm{E}\left\{\left|\mathbf{W}_{(u,u)}\right|^{-4}\right\} = \frac{1}{B_1}. \tag{61}$$

Hence we complete the proof of ***Lemma 1***.

C. Proof of ***Lemma 2***

For $u \in \mathbb{U}_2$, $v = u-1$, from Equation (22), we have

$$\mathbf{B}_{(u,u-1)} = \frac{\mathbf{G}_{(u,u+1)}\mathbf{G}_{(u+1,u-1)}}{\mathbf{G}_{(u,u)}\mathbf{G}_{(u+1,u+1)}}.$$

Applying the Cauchy-Schwarz inequality, we have

$$\begin{aligned}\mathrm{E}\left\{\left|\mathbf{B}_{(u,u-1)}\right|^2\right\} &\leqslant \sqrt{\mathrm{E}\left\{\left|\mathbf{G}_{(u,u+1)}\mathbf{G}_{(u+1,u-1)}\right|^4\right\}} \\ &\cdot\sqrt{\mathrm{E}\left\{\left|\left(\mathbf{G}_{(u,u)}\mathbf{G}_{(u+1,u+1)}\right)^{-1}\right|^4\right\}}\end{aligned} \tag{62}$$

According to ***Lemma 8*** and ***Lemma 6***, we have

$$\mathrm{E}\left\{\left|\mathbf{G}_{(u,u+1)}\mathbf{G}_{(u+1,u-1)}\right|^4\right\} = A_2, \tag{63}$$

$$\begin{aligned}\mathrm{E}\left\{\left|\left(\mathbf{G}_{(u,u)}\mathbf{G}_{(u+1,u+1)}\right)^{-1}\right|^4\right\} &= \mathrm{E}\left\{\left|\left(\mathbf{G}_{(u,u)}\right)^{-1}\right|^4\right\} \\ &\cdot\mathrm{E}\left\{\left|\left(\mathbf{G}_{(u,u)}\right)^{-1}\right|^4\right\} \\ &= \frac{1}{B_1^2}.\end{aligned} \tag{64}$$

For $u \in \mathbb{U}_2$, $v = u+1$, following the similar process, we have the same result above. Therefore, we complete the proof of ***Lemma 2***.

$$\begin{aligned}\mathrm{E}\left\{\left|\mathbf{B}_{(u,v)}\right|^2\right\} &= \mathrm{E}\left\{\frac{\left|\mathbf{G}_{(u+1,u+1)}\mathbf{G}_{(u,u-1)}\mathbf{G}_{(u-1,v)} + \mathbf{G}_{(u-1,u-1)}\mathbf{G}_{(u,u+1)}\mathbf{G}_{(u+1,v)} - \mathbf{G}_{(u-1,u-1)}\mathbf{G}_{(u+1,u+1)}\mathbf{G}_{(u,v)}\right|^2}{\left|\mathbf{G}_{(u-1,u-1)}\mathbf{G}_{(u,u)}\mathbf{G}_{(u+1,u+1)}\right|^2}\right\} \\ &\leqslant \sqrt{\mathrm{E}\left\{\left|\mathbf{G}_{(u+1,u+1)}\mathbf{G}_{(u,u-1)}\mathbf{G}_{(u-1,v)} + \mathbf{G}_{(u-1,u-1)}\mathbf{G}_{(u,u+1)}\mathbf{G}_{(u+1,v)} - \mathbf{G}_{(u-1,u-1)}\mathbf{G}_{(u+1,u+1)}\mathbf{G}_{(u,v)}\right|^4\right\}} \\ &\quad \cdot \sqrt{\mathrm{E}\left\{\left|\mathbf{G}_{(u-1,u-1)}\mathbf{G}_{(u,u)}\mathbf{G}_{(u+1,u+1)}\right|^{-4}\right\}}\end{aligned} \tag{65}$$

$$\begin{aligned}&\mathrm{E}\left\{\left|\mathbf{G}_{(u+1,u+1)}\mathbf{G}_{(u,u-1)}\mathbf{G}_{(u-1,v)} + \mathbf{G}_{(u-1,u-1)}\mathbf{G}_{(u,u+1)}\mathbf{G}_{(u+1,v)} - \mathbf{G}_{(u-1,u-1)}\mathbf{G}_{(u+1,u+1)}\mathbf{G}_{(u,v)}\right|^4\right\} \\ &= \mathrm{E}\left\{(A+B+C+D+E+F)^2\right\} \leqslant 6\mathrm{E}\left\{A^2+B^2+C^2+D^2+E^2+F^2\right\}\end{aligned} \tag{66}$$

$$\mathrm{E}\left\{D^2\right\} \leqslant 4\mathrm{E}\left\{\left|\mathbf{G}_{(u+1,u+1)}\mathbf{G}_{(u-1,u-1)}\mathbf{G}_{(u,u-1)}\mathbf{G}_{(u-1,v)}\mathbf{G}^*_{(u,u+1)}\mathbf{G}^*_{(u+1,v)}\right|^2\right\} = 4A_4 \tag{69}$$

$$\begin{aligned}\mathrm{E}\left\{\left|\mathbf{B}_{(u,u)}\right|^2\right\} &= \mathrm{E}\left\{\frac{\left|\mathbf{G}_{(u+1,u+1)}\left|\mathbf{G}_{(u,u-1)}\right|^2 + \mathbf{G}_{(u-1,u-1)}\left|\mathbf{G}_{(u,u+1)}\right|^2\right|^2}{\left|\mathbf{G}_{(u,u)}\mathbf{G}_{(u-1,u-1)}\mathbf{G}_{(u+1,u+1)}\right|^2}\right\} \\ &\leqslant \sqrt{\mathrm{E}\left\{\left|\mathbf{G}_{(u+1,u+1)}\left|\mathbf{G}_{(u,u-1)}\right|^2 + \mathbf{G}_{(u-1,u-1)}\left|\mathbf{G}_{(u,u+1)}\right|^2\right|^4\right\} \cdot \mathrm{E}\left\{\left|\mathbf{G}_{(u,u)}\mathbf{G}_{(u-1,u-1)}\mathbf{G}_{(u+1,u+1)}\right|^{-4}\right\}}\end{aligned} \tag{73}$$

---

*D. Proof of **Lemma 3***

For $u \in \mathbb{U}_2$, $v \notin \{u-1, u, u+1\}$, from Equation (22), we have $\mathrm{E}\left\{\left|\mathbf{B}_{(u,v)}\right|^2\right\}$ given by Equation (65), where the Cauchy-Schwarz inequality is applied. Next, we have the first expectation in the right hand side of the inequality (65) given by (66), where

$$\begin{aligned}A &= \left|\mathbf{G}_{(u+1,u+1)}\right|^2\left|\mathbf{G}_{(u,u-1)}\mathbf{G}_{(u-1,v)}\right|^2, \\ B &= \left|\mathbf{G}_{(u-1,u-1)}\right|^2\left|\mathbf{G}_{(u,u+1)}\mathbf{G}_{(u+1,v)}\right|^2, \\ C &= \left|\mathbf{G}_{(u-1,u-1)}\right|^2\left|\mathbf{G}_{(u+1,u+1)}\right|^2\left|\mathbf{G}_{(u,v)}\right|^2, \\ D &= 2\,\mathrm{Re}\left(\mathbf{G}_{(u,u-1)}\mathbf{G}_{(u-1,v)}\mathbf{G}^*_{(u,u+1)}\mathbf{G}^*_{(u+1,v)}\right) \\ &\quad \cdot \mathbf{G}_{(u+1,u+1)}\mathbf{G}_{(u-1,u-1)}, \\ E &= -2\,\mathrm{Re}\left(\mathbf{G}_{(u,u-1)}\mathbf{G}_{(u-1,v)}\mathbf{G}^*_{(u,v)}\right) \\ &\quad \cdot \left|\mathbf{G}_{(u+1,u+1)}\right|^2\mathbf{G}_{(u-1,u-1)}, \\ F &= -2\,\mathrm{Re}\left(\mathbf{G}_{(u,u+1)}\mathbf{G}_{(u+1,v)}\mathbf{G}^*_{(u,v)}\right) \\ &\quad \cdot \left|\mathbf{G}_{(u-1,u-1)}\right|^2\mathbf{G}_{(u+1,u+1)}.\end{aligned}$$

The inequality (66) holds by noting that

$$\begin{aligned}&(A+B+C+D+E+F)^2 \\ &\leqslant 6\left(A^2+B^2+C^2+D^2+E^2+F^2\right),\end{aligned}$$

where A, B, C, D, E, F are both real numbers. Next, we derive the expectations as follows individually.

With the results in ***Lemma 6*** and ***Lemma 8***, we have $\mathrm{E}\left(A^2\right) = \mathrm{E}\left(B^2\right)$ given by

$$\mathrm{E}\left(A^2\right) = \mathrm{E}\left(B^2\right) = A_2A_3. \tag{67}$$

$\mathrm{E}\left(C^2\right)$ is given by

$$\mathrm{E}\left\{C^2\right\} = A_1{A_3}^2. \tag{68}$$

where the results in ***Lemma 6*** and ***Lemma 7*** are applied.

By using $(\mathrm{Re}\,(a))^2 \leqslant |a|^2$, we derive the result of $\mathrm{E}\left\{D^2\right\}$, given by (69), where A_4 is obtained through ***Lemma 9***.

Applying the Cauchy-Schwarz inequality, we have

$$\begin{aligned}\mathrm{E}\left\{E^2\right\} &\leqslant 4\mathrm{E}\left\{\left|\mathbf{G}_{(u-1,u-1)}\mathbf{G}_{(u,u-1)}\mathbf{G}_{(u-1,v)}\mathbf{G}^*_{(u,v)}\right|^2\right\} \\ &\quad \cdot \mathrm{E}\left\{\left|\mathbf{G}_{(u+1,u+1)}\right|^4\right\} \\ &\leqslant 4\mathrm{E}\left\{\left|\mathbf{G}_{(u+1,u+1)}\right|^4\right\}\sqrt{\mathrm{E}\left\{\left|\mathbf{G}_{(u,u-1)}\mathbf{G}_{(u-1,v)}\right|^4\right\}} \\ &\quad \cdot \sqrt{\mathrm{E}\left\{\left|\mathbf{G}_{(u-1,u-1)}\mathbf{G}_{(u,v)}\right|^4\right\}}\end{aligned} \tag{70}$$

With the results in ***Lemma 6***, ***Lemma 7***, and ***Lemma 8***, we derive the result of $\mathrm{E}\left\{E^2\right\} = \mathrm{E}\left\{F^2\right\}$, given by

$$\mathrm{E}\left\{E^2\right\} = \mathrm{E}\left\{F^2\right\} \leqslant 4A_3\sqrt{A_1A_2A_3}. \tag{71}$$

Therefore, we derive

$$\mathrm{E}\left\{\left|\mathbf{B}_{(u,v)}\right|^2\right\} \leqslant \sqrt{\frac{12A_2A_3 + 6A_1A_3^2 + 24A_4 + 48\sqrt{A_1A_2A_3^3}}{B_1^3}} \tag{72}$$

Hence, we complete the proof of ***Lemma 3***.

*E. Proof of **Lemma 4***

For $u \in \mathbb{U}_2$, $v = u$, from Equation (22), we have $\mathrm{E}\left\{\left|\mathbf{B}_{(u,v)}\right|^2\right\}$ given by (73), where the Cauchy-Schwarz inequality is applied. By using $|a+b|^2 \leqslant 2\left(|a|^2+|b|^2\right)$, we have

$$\begin{aligned}
&\left|\mathbf{G}_{(u+1,u+1)}\left|\mathbf{G}_{(u,u-1)}\right|^2+\mathbf{G}_{(u-1,u-1)}\left|\mathbf{G}_{(u,u+1)}\right|^2\right|^2 \\
&\leqslant 2\left(\left|\mathbf{G}_{(u+1,u+1)}\right|^2\left|\mathbf{G}_{(u,u-1)}\right|^4+\left|\mathbf{G}_{(u-1,u-1)}\right|^2\left|\mathbf{G}_{(u,u+1)}\right|^4\right), \\
&\left|\mathbf{G}_{(u+1,u+1)}\left|\mathbf{G}_{(u,u-1)}\right|^2+\mathbf{G}_{(u-1,u-1)}\left|\mathbf{G}_{(u,u+1)}\right|^2\right|^4 \\
&\leqslant 8\left(\left|\mathbf{G}_{(u+1,u+1)}\right|^4\left|\mathbf{G}_{(u,u-1)}\right|^8+\left|\mathbf{G}_{(u-1,u-1)}\right|^4\left|\mathbf{G}_{(u,u+1)}\right|^8\right).
\end{aligned} \tag{74}$$

Therefore, we derive

$$\begin{aligned}
&\mathrm{E}\left\{\left|\mathbf{G}_{(u+1,u+1)}\left|\mathbf{G}_{(u,u-1)}\right|^2+\mathbf{G}_{(u-1,u-1)}\left|\mathbf{G}_{(u,u+1)}\right|^2\right|^4\right\} \\
&\leqslant 8\mathrm{E}\left(\left|\mathbf{G}_{(u+1,u+1)}\right|^4\right)\mathrm{E}\left(\left|\mathbf{G}_{(u,u-1)}\right|^8\right) \\
&\quad+8\mathrm{E}\left(\left|\mathbf{G}_{(u-1,u-1)}\right|^4\right)\mathrm{E}\left(\left|\mathbf{G}_{(u,u+1)}\right|^8\right).
\end{aligned} \tag{75}$$

With the results in ***Lemma 6*** and ***7***, we have

$$\mathrm{E}\left\{\left|\mathbf{B}_{(u,u)}\right|^2\right\} \leqslant \sqrt{\frac{16A_3A_5}{B_1^3}}. \tag{76}$$

Hence we complete the proof of ***Lemma 4***.

References

[1] T. Marzetta, "Noncooperative Cellular Wireless with Unlimited Numbers of Base Station Antennas," *IEEE Transactions on Wireless Communications*, vol. 9, no. 11, pp. 3590–3600, Nov. 2010.

[2] F. Rusek, D. Persson, B. Lau, E. Larsson, T. Marzetta, O. Edfors, and F. Tufvesson, "Scaling Up MIMO: Opportunities and Challenges with Very Large Arrays," *IEEE Signal Processing Magazine*, vol. 30, no. 1, pp. 40–60, Jan. 2013.

[3] E. Larsson, O. Edfors, F. Tufvesson, and T. Marzetta, "Massive MIMO for Next Generation Wireless Systems," *IEEE Communications Magazine*, vol. 52, no. 2, pp. 186–195, Feb. 2014.

[4] T. Rappaport, S. Sun, R. Mayzus, H. Zhao, Y. Azar, K. Wang, G. W. J. Schulz, M. Samimi, and F. Gutierrez, "Millimeter Wave Mobile Communications for 5G Cellular: It Will Work!" *IEEE Access*, vol. 1, pp. 335–349, May 2013.

[5] H. Ngo, E. Larsson, and T. Marzetta, "Energy and Spectral Efficiency of Very Large Multiuser MIMO Systems," *IEEE Transactions on Communications*, vol. 61, no. 4, pp. 1436–1449, Apr. 2013.

[6] J. Hoydis, S. Brink, and M. Debbah, "Massive MIMO in the UL/DL of Cellular Networks: How Many Antennas Do We Need?" *IEEE Journal on Selected Areas in Communications*, vol. 31, no. 2, pp. 160–171, Feb. 2013.

[7] E. Bjornson, L. Sanguinetti, J. Hoydis, and M. Debbah, "Optimal Design of Energy-Efficient Multi-User MIMO Systems: Is Massive MIMO the Answer?" *IEEE Transactions on Wireless Communications*, vol. 14, no. 6, pp. 3059–3075, Jun. 2015.

[8] M. Wu, B. Yin, G. Wang, C. Dick, J. Cavallaro, and C. Studer, "Large-Scale MIMO Detection for 3GPP LTE: Algorithms and FPGA Implementations," *IEEE Journal of Selected Topics in Signal Processing*, vol. 8, no. 5, pp. 916–929, Mar. 2014.

[9] D. Zhu, B. Li, and P. Liang, "On the Matrix Inversion Approximation Based on Neumann Series in Massive MIMO Systems," in *Proceedings of the IEEE International Conference on Communications*, London, UK, Jun. 2015, pp. 1763–1769.

[10] C. Tang, C. Liu, L. Yuan, and Z. Xing, "High Precision Low Complexity Matrix Inversion Based on Newton Iteration for Data Detection in the Massive MIMO," *IEEE Communications Letters*, vol. 20, no. 3, pp. 490–493, Mar. 2016.

[11] F. Wang, C. Zhang, X. Liang, Z. Wu, S. Xu, and X. You, "Efficient Iterative Soft Detection Based on Polynomial Approximation for Massive MIMO," in *Proceedings of the IEEE International Conference on Wireless Communications and Signal Processing*, Nanjing, China, Oct. 2015, pp. 1–5.

[12] X. Gao, L. Dai, Y. Ma, and Z. Wang, "Low-complexity near-optimal signal detection for uplink large scale MIMO systems," *Electronics Letters*, vol. 50, no. 18, pp. 1326–1328, Aug. 2014.

[13] L. Dai, X. Gao, X. Su, S. Han, C. I, and Z. Wang, "Low-Complexity Soft-Output Signal Detection Based on Gauss-Seidel Method for Uplink Multiuser Large-Scale MIMO Systems," *IEEE Transactions on Vehicular Technology*, vol. 64, no. 10, pp. 4839–4845, Oct. 2015.

[14] X. Qin, Z. Yan, and G. He, "A Near-Optimal Detection Scheme Based on Joint Steepest Descent and Jacobi Method for Uplink Massive MIMO Systems," *IEEE Communications Letters*, vol. 20, no. 2, pp. 276–279, Feb. 2016.

[15] B. Yin, M. Wu, J. Cavallaro, and C. Studer, "Conjugate Gradient-based Soft-output Detection and Precoding in Massive MIMO Systems," in *Proceedings of the IEEE Global Communications Conference*, Austin, TX, USA, Dec. 2014, pp. 3696–3701.

[16] J. Burgerscentrum, "Iterative Solutions Methods," *Applied Numerical Mathematics*, vol. 51, no. 4, pp. 437–450, 2011.

[17] F. Jiang, C. Li, and Z. Gong, "A Low Complexity Soft-output Data Detection Scheme Based on Jacobi Method for Massive MIMO Uplink Transmission," in *Proceedings of the IEEE International Conference on Communications*, Paris, France, May 2017, to appear.

[18] L. Dai, Z. Wang, and Z. Yang, "Spectrally Efficient Time-Frequency Training OFDM for Mobile Large-Scale MIMO Systems," *IEEE Journal on Selected Areas in Communications*, vol. 31, no. 2, pp. 251–263, Feb. 2013.

[19] Z. Gao, L. Dai, W. Dai, B. Shim, and Z. Wang, "Structured Compressive Sensing-Based Spatio-Temporal Joint Channel Estimation for FDD Massive MIMO," *IEEE Transactions on Communications*, vol. 64, no. 2, pp. 601–617, Feb. 2016.

[20] H. Lou, "Stair Matrices and Their Generalizations with Applications to Iterative Methods I: A Generalization of the Successive Overrelaxation Method," *SIAM Journal on Numerical Analysis*, vol. 37, no. 1, pp. 1–17, 2000.

[21] H. Li, T. Huang, Y. Zhang, X. Liu, and T. Gu, "Chebyshev-type Methods and Preconditioning Techniques," *Applied Mathematics and Computation, Elsevier*, vol. 218, no. 2, pp. 260–270, 2011.